AFRL-VS-TR-2000-1516

IRRADIANCE CALIBRATION OF SPACE-BASED INFRARED SENSORS

Russell Walker
Martin Cohen

Vanguard Research, Inc.
5321 Scotts Valley Drive, Suite 204
Scotts Valley, CA 95066

July 1999

Scientific Report No. 1

AIR FORCE RESEARCH LABORATORY
Space Vehicles Directorate
29 Randolph Rd
AIR FORCE MATERIEL COMMAND
HANSCOM AFB, MA 01731-3010

20031126 108

This technical report has been reviewed and is approved for publication.

/Signed/
TAMALYN BECKER, 2ND Lt, USAF
Contract Manager

/Signed/
ROBERT BELAND
Branch Chief

REPORT DOCUMENTATION PAGE

1. REPORT DATE *(DD-MM-YYYY)*	2. REPORT TYPE	3. DATES COVERED *(From - To)*
xx-07-1999	Scientific Report No. 1	May 1998-July 1999

4. TITLE AND SUBTITLE

Irradiance Calibration of Space-Based Infrared Sensors, Annual Report No. 1

5a. CONTRACT NUMBER

C F19628-98-C-0047

5b. GRANT NUMBER

5c. PROGRAM ELEMENT NUMBER

PE 63871 C

6. AUTHOR(S)

Russell G. Walker and Martin Cohen

5d. PROJECT NUMBER

PR MSX8

5e. TASK NUMBER

TA-BS

5f. WORK UNIT NUMBER

WU AE

7. PERFORMING ORGANIZATION NAME(S) AND ADDRESS(ES)

Vanguard Research, Inc.
5321 Scotts Valley Drive, Suite 204
Scotts Valley, CA 95066

8. PERFORMING ORGANIZATION REPORT NUMBER

VRISV-1130-AR03

9. SPONSORING/MONITORING AGENCY NAME(S) AND ADDRESS(ES)

Air Force Research Laboratory/VSBYH
20 Randolph Road
Hanscom AFB, MA, 01731-3-1-

10. SPONSOR/MONITOR'S ACRONYM(S)

AFRL-VS-TR

11. SPONSOR/MONITOR'S REPORT NUMBER(S)

2000-1516

12. DISTRIBUTION/AVAILABILITY STATEMENT

Approved for Public Release; Distribution Unlimited.

13. SUPPLEMENTARY NOTES

14. ABSTRACT

Abstract

The purpose of this work is to develop a basis for irradiance calibration of space-based sensors. It is an extension of previous work that fully defines the context of calibration, and the concepts of spectral composites and templates. We discuss two areas of work carried out during the past year; our accomplishments and failures; and our plans for the future. The two areas are:
1) A description of the Celestial Backround Experiment CB06
2) Production of the preliminary Air Force Bright Spectral Catalog

15. SUBJECT TERMS

IR Sources, Infrared, Calibration, Spectra, Stars

16. SECURITY CLASSIFICATION OF:			17. LIMITATION OF ABSTRACT	18. NUMBER OF PAGES	19a. NAME OF RESPONSIBLE PERSON
a. REPORT	b. ABSTRACT	c. THIS PAGE	UL	26	2Lt Tamilyn Becker
U	U	U			19b. TELEPHONE NUMBER *(Include area code)* (781)377-3696

Table of Contents

Figures and Tables

1. Introduction

Satellites employing infrared sensors are continually being launched by space agencies, such as NASA and ESA and by the US DOD community. The successes of IRAS, ISO, IRTS, and MSX have already produced enormous infrared databases. Consequently, there must now be greater emphasis on data verification, validation, and calibration issues to assure that these data sets are of sufficient reliability for application to the quantitative design of advanced spaceborne sensors and systems. There is an urgent need not only to rationalize infrared calibration and place it in a common and well-defined context, but also to provide a network of calibrators well distributed across the sky, with a common traceable pedigree. This network should be sufficiently populated to have a member relatively close to any arbitrary direction because satellites and aircraft cannot afford major excursions in pointing to secure measurements of the few traditional calibration objects. Dynamic range, too, is an issue and such a network must include stars both fainter and brighter than today's popular "standards".

The purpose of this work is to develop a basis for irradiance calibration of space-based infrared sensors. It is an extension of previous work (Cohen, et al. Papers I-IX, 1992-1998) that fully defines the context of the calibration, and the concepts of spectral composites and templates. This work culminated in the recent publication *of A Self-Consistent Radiometric All-Sky Network of Absolutely Calibrated Stellar Spectra* (Cohen, et al. Paper X, 1999). Our approach is based on a self-consistent absolute framework within which radiometry and spectroscopy are unified, with wavelength coverage ideal for calibrating many satellite, airborne, and ground-based sensors.

In the above series of papers we have described a consistent effort to provide absolutely calibrated broad and narrowband IR photometry based upon a carefully selected, IR-customized pair of absolutely calibrated stellar models for the A-stars, Vega and Sirius. These hot stellar models have been employed as reference spectra to calibrate the spectra of cool (K0-M0) giants. This approach has yielded a valuable set of secondary stellar standards with calibration pedigrees directly traceable to the two primary standards. These cool giant spectra are totally unlike any blackbody, and are dominated by the fundamental absorption and overtones of CO, SiO, and water vapor. Thus the ideal (IR-bright) calibrators have significant spectral structure that is not yet adequately modeled by stellar atmospheric codes but that can be approached in a rigorous observational manner. These (almost) entirely observed 1.2-35 μm absolute spectra of all reference stars are designated "composite spectra" (because of the method of their assembly). Our self-consistent calibration assures one derives the identical conversion from instrumental quantities to physical units *whichever* star is used.

Each composite spectrum can be used to create many calibrated stellar spectra, all with a traceable common calibration heritage, given a single prerequisite, namely photometry in a "well-characterized" system of filters. To achieve this goal, one must make the fundamental "template assumption", that the dereddened (for interstellar extinction) infrared spectral shape of any observed K0-M0 giant accurately represents the intrinsic spectrum of any other giant with the same two-dimensional spectral type as the composite from which the "template" is created. The adopted template (spectral shape) is reddened appropriately for the star to be templated in the IR, then normalized by matching the template's in-band radiometry to the measured in-band irradiances in a set of filters. The *All Sky Network of 422 Infrared Calibration Stars* referenced above was produced using this technique.

1

The present, ongoing work is divided into two areas:

a) Data from the MSX/SPIRIT III CB06 celestial background calibration experiments is being reduced, validated, and analyzed to produce a sub-network of calibration stars that will be integrated into the current network. This sub-network will be used to provide an independent check on the internal consistency of the infrared spectral templates used in the network, as well as add several new stars to the present network.

b) Data from the literature are being assembled and analyzed to produce an independent set of calibrators selected to be among the IR-brightest sources in the sky rather than sources of a specific optical type. This Air Force Bright Spectral Catalog (AFBSC) is particularly relevant to space-based programs, such as SBIRS, and to ground-based programs in the 20 µm spectral region such as those to begin soon at AMOS using the new Philips Laboratory 3.5 meter telescope.

This report describes the methods, assumptions, and procedures that we are using to accomplish the above work; and summarizes its present status and accomplishments.

2. Celestial Background Experiment CB06 – Absolute Calibration
2.1 The Experiment

SPIRIT III carried out a number of radiometric investigations of the composites, intercomparing ground calibration, on-orbit calibration via the "emissive spheres" experiments, and the stellar calibrations. Preliminary analyses (*e.g.* Murdock 1997) of the reference spheres' experiments already indicate good agreement between the three approaches to on-orbit calibration of MSX. These results validate our composites in the sense that the observed radiometric ratios of one stellar spectrum to another match our expectations at the 1σ uncertainty level in all SPIRIT III bands.

We are currently analyzing one of the stellar calibration experiments from MSX, namely the "triads" of the experiment "CB06". In these, we made raster-scan observations of three stars using the SPIRIT III radiometers. Two stars, usually from our network of 422 template stars, were selected for measurement and, between them, we made identical observations of a bright reference star (composite). The three sets of observations were contained within a single Data Collection Event (DCE) lasting about 35 minutes, to minimize changes in sensor performance. Each star was raster-scanned 18 to 20 times with a small offset in the cross-scan direction between scans. The star was initially observed with the lower third of the detector array column, but was switched to the upper third after scan 10 to enable sampling of both B Bands.

The triads perform three functions. First, if we accept the absolute calibration imposed by the pipeline processing of these MSX data, we can examine the implied in-band irradiances of our stellar composites in all the SPIRIT III bands. Preliminary indications suggest that our published spectra provide irradiances within only a few percent of those derived from the CB06 events. Second, each event provides relative radiometry on one or two elements in our network of calibrators with which we can test directly the calibrated templates. We have chosen a few stars for which we have carefully characterized ground-based photometry already so we can validate the scale factors for these particular templates with and without SPIRIT III data. Third, we have included several stars of known spectral type that can be used to expand the calibration network. In addition, several target stars were included in

2

multiple events as a further check on SPIRIT III reproducibility. Using these data we will create a subnetwork of radiometric standards based solely on MSX data.

2.2 The Observations

A total of 24 DCEs were successfully carried out for the CB06 experiment. Table 1 gives a brief summary of the circumstances for these observations: the abbreviated observation number, the date of the observation, the three stars observed, and the temperature range of the SPIRIT III focal plane (Band B) during the DCE. Temperatures in parentheses are estimated. The list contains multiple observations of 9 stars with composite spectra, 34 with template spectra (8 with only IRAS photometry, 17 with IRAS + IRC photometry, and 9 with photometry from 3 or more groups), and 2 new stars. All are potential members of the MSX-based subnetwork.

Most of the observations were taken late in the MSX mission when the focal plane temperature was higher than the nominal 11K that was anticipated, increasing the noise and dark offset of the arrays and limiting the useful dynamic range. This can be expected to have two effects on our results: 1) some faint sources will not be detected in all spectral bands, and 2) increased noise and less stability of response will increase the uncertainties of the measurements.

Table 1. Circumstances of the CB06 Observations.					
Observation	Date	Star 1	Star 2	Star 3	Temperature
CB0604	06-21-96	γ CRU	α BOO	β PEG	11.200-11.330
CB0605	07-03-96	α BOO	γ DRA	α LYR	11.380-11.430
CB0606	10-08-96	SAO248381	α LYR	42 DRA	11.500-11.580
CB0607	10-14-96	IRC+50004	SAO783	β GEM	11.840-11.970
CB0608	12-31-96	α ARI	β AND	4 UMI	12.030-11.940
CB0609	01-14-97	60 AND	α TAU	16 AUR	12.050-12.230
CB0610	01-20-97	SAO195639	α CMA	45 ERI	12.150-12.250
CB0613	01-27-97	GL4509S	α CMA	π6 ORI	12.230-12.410
CB0614	01-28-97	31 ORI	α TAU	40 CAM	12.230-12.410
CB0615	01-29-97	β COL	α TAU	ι AUR	12.200-12.330
CB0616	02-01-97	β VOL	α CMA	24 PER	12.360-12.540
CB0617	02-02-97	γ2 VOL	α CMA	τ2 ARI	12.230-12.150
CB0618	02-04-97	δ LEP	α CMA	31 ORI	(12.2-12.5)
CB0619	02-04-97	δ LEP	α CMA	45 ERI	(12.2-12.5)
CB0620	02-03-97	24 COM	α BOO	SAO250019	(12.2-12.5)
CB0621	02-08-97	SAO223297	α CMA	τ2 ARI	(12.2-12.5)
CB0622	02-10-97	6 DRA	α BOO	SAO222136	(12.3-12.6)
CB0623	02-15-97	SAO249451	α CMA	56 ORI	(12.3-12.6)
CB0624	02-16-97	γ PIC	α CMA	45 ERI	(12.3-12.6)
CB0625	02-24-97	ρ SER	α BOO	51 HYA	(12.4-12.7)
CB0626	02-25-97	ρ SER	α BOO	51 HYA	(12.4-12.7)
CB0631	02-25-97	26 LYN	α BOO	IRC+10266	(12.4-12.7)
CB0632	02-26-97	6 PUP	α CMA	18 MON	(12.4-12.7)
CB0633	02-26-97	32 COM	α BOO	SAO250979	(12.4-12.7)

2.3 Data Processing and Analysis
2.3.1 CONVERT Processing

Our basic inputs are Level 1A Exabyte data tapes, which for all the CB06 DCEs were received from the Phillips Laboratory (PL) Data Analysis Center (DAC), and MSX Definitive Attitude Files (DAF) which we downloaded from the Science Catalog Information Exchange System (SCIES). These data sets are then processed by a SGI INDIGIO computer through CONVERT 6.22 and using the appropriate instrument products to produce Level 2A extended source files. CONVERT is run with all the input parameters set to produce a certified output. The dead pixel mask provided with the Level 1A data tape is used.

The DAF is then used to determine the limits (turnaround times) of each scan across the target star. These times are subsequently input to create a PERL script that controls the processing through POINTING CONVERT 6.0. The Level 2A extended source files are then processed through POINTING to create a time and position tagged extended source *.MAP file for each scan of each star. Once the *.MAP files have been created and archived on tape the processing continues using analysis software.

We initially tried to use the point source extraction feature of CONVERT and found that it produced unacceptable photometric reproducibility from scan to scan. We believe that this is a consequence of the continually varying scan velocity throughout the CB06 scans, and not a fault with the CONVERT source extractor. The CONVERT source extractor creates an image in focal plane coordinates and requires a constant scan velocity to function properly. For this reason we have chosen to construct images in celestial coordinates for each scan, and apply aperture photometry to estimate the point source irradiance.

2.3.2 Image Construction

The IDL procedure CB06FINAL creates an image of each scan in a $3° \times 3°$ window centered on the targeted star. The coordinates are Right Ascension (RA) and Declination (Dec), and the pixel size is 9 seconds of arc. The window is larger than the nominal $1° \times 0.75°$ scanned region to allow for an arbitrary scan angle, cross-scan steps, and the shift from observing the star in the upper third of the detector columns to the lower third.

Once a *.MAP file (1 star, 1 scan, 1 spectral band) has been read into memory, a single (virtual) column image is created and the noise and residual dark offset and background radiance is measured for each pixel of the column. This is repeated for each column in the detector array for that band. A column image is simply the time history of the pixels' responses during the scan. The noise is estimated by the procedure described in the Appendix. It is important to note that the noise estimated here is essentially the sum of the dark noise, the photon noise from the mean background, and any noise due to radiance structure in the background. It does not include a significant amount of photon noise from bright sources. This procedure was successfully used for processing the SPIRIT III data from the DC34 experiments for the Space Dynamics Laboratory (Walker, 1998). Dark offset and background radiance are not separated, but estimated as a total baseline offset. Fitting a first or second order polynomial by the method of least squares to the pixel time history does this. The linear fit is used for observations in SPIRIT III integration modes EL16 and EL16+ due to the poor noise statistics. The effects of stars and glitches are minimized by iteration of the baseline fit after removal of all signals with amplitude greater than a 2.5σ threshold. Thus
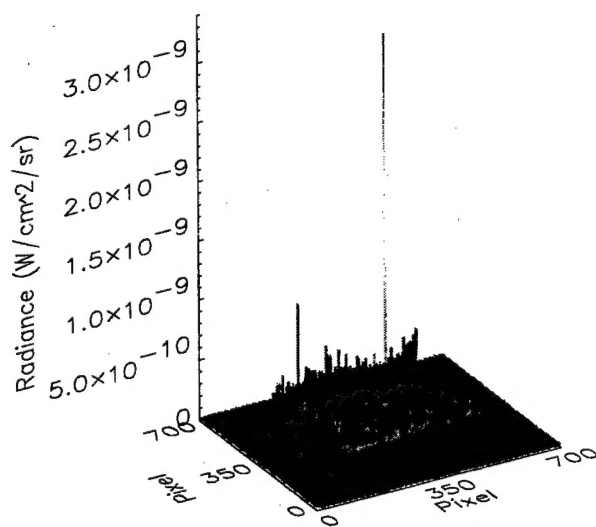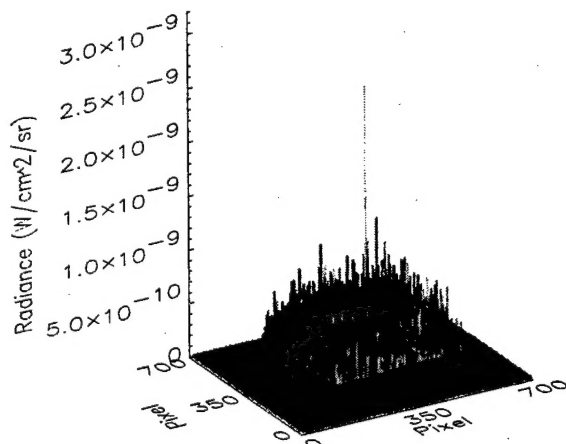
4
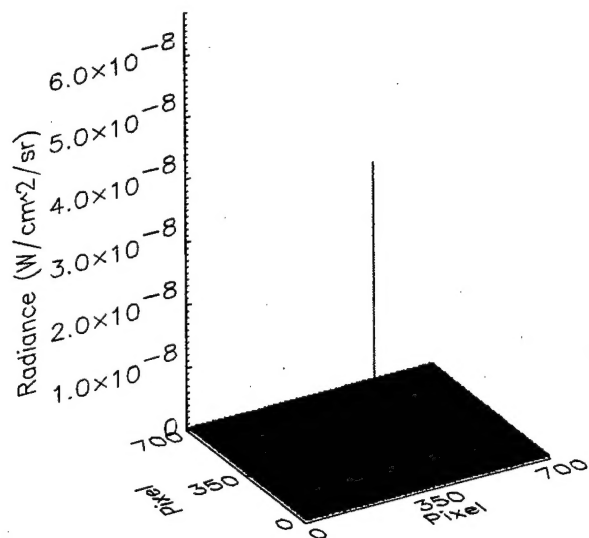
BAND A
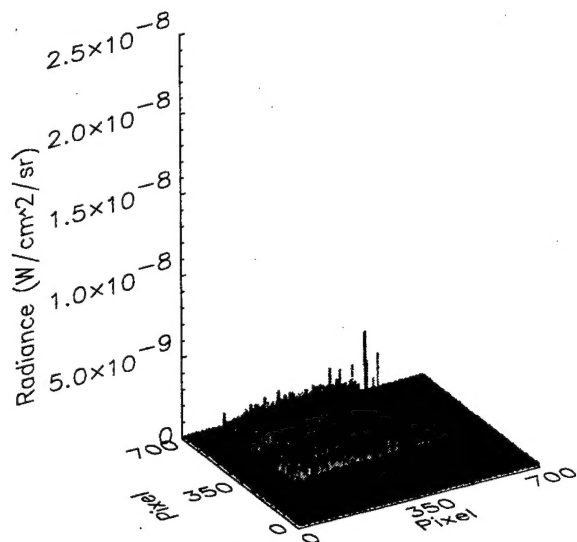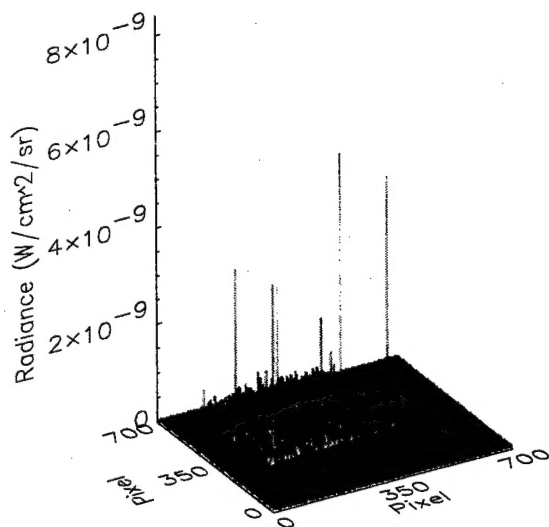
BAND B2

BAND C

BAND D

BAND E

Figure 1. Single scan images of α Lyr from CB0605 scan 7. The star is located at pixel (350,350). Several strong single pixel events can be seen in Bands B, C and D.

each pixel sample now has an associated noise and baseline offset. Pixels with excessive noise are flagged and not processed for image construction. Table 2 lists those consistently noisy pixels that have been removed from all of our data sets.

Table 2. Noisy pixels that were removed from all DCEs.		
Band	Column	Pixel Number (CONVERT Numbering Convention)
B	1	46, 47, 66, 67, 68, 69, 83, 84, 103, 104, 105, 106
B	2	66, 67, 68, 83, 84, 102, 103, 104, 105, 106
D	2	35, 129
D	4	129

Valid pixel samples are baseline subtracted, weighted according to their inverse variance, and binned into the image array according to their RA and DEC coordinates. Images of both the radiance and the standard deviation of the radiance are constructed. Sub-images 1.75^0 x 1.75^o centered on the target star are selected and written to *.FITS files. Plots of typical single scan images are given in Figure 1 (a, b, c, d, e) for the standard star α Lyr.

2.3.3 Photometry of the Stars

The procedure PHOTOMETER_CB06 performs aperture photometry of the target stars. The FITS images from CB06FINAL are read by the procedure, cleaned of any single pixel events (spikes) that may be present, and sub-arrays that are 101 x 101 pixels centered on the star are selected for photometry.

Aperture photometry is implemented using two techniques, 1) the curve of growth method and 2) the photometric profile method. The curve of growth method sums the radiance within a set of circular apertures of increasing radius centered on the star. If the baseline is truly zero, in the absence of noise, the curve of growth will reach an asymptotic value when all the flux from the star has been included. The value of the asymptote can be taken as a measure of the brightness of the star. This method is useful for bright stars observed at a high signal to noise ratio (SNR). A typical set of curves of growth is shown in Figure 2.

For faint stars the addition of the noise at large radii dominates the curve of growth process. The peak SNR for stars observed by SPIRIT III usually occurs at a radius of about 3 pixels from the star. The photometric profile method relies on the assumption that the shape of the curve of growth is determined only by the point response function (PRF) of the telescope-detector system. Therefore, a measurement of the flux at optimum SNR can be corrected to the asymptotic value of the flux using the known curve of growth. Photometric profiles for each band were derived from 3 observations of α Tau and 8 of α Boo, the brightest stars in our set. Figure 3 shows the data used and the resulting templates for the SPIRIT III bands.

In practice the mean baseline of the sub-array is never exactly zero and an asymptote will never be reached. The curve will continue to rise if the residual is positive and roll-over and
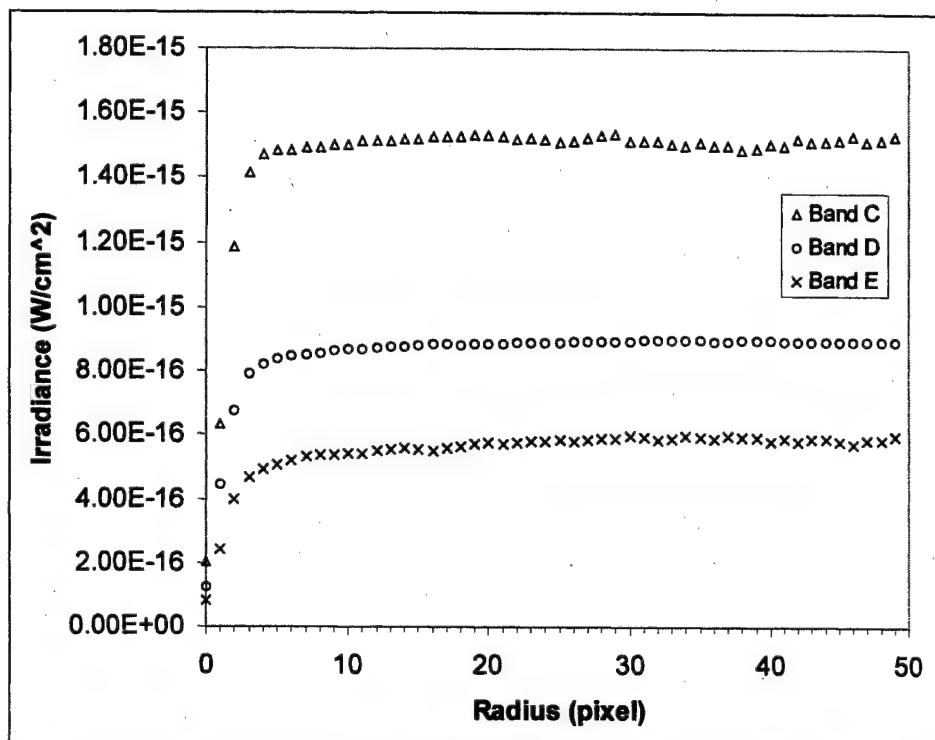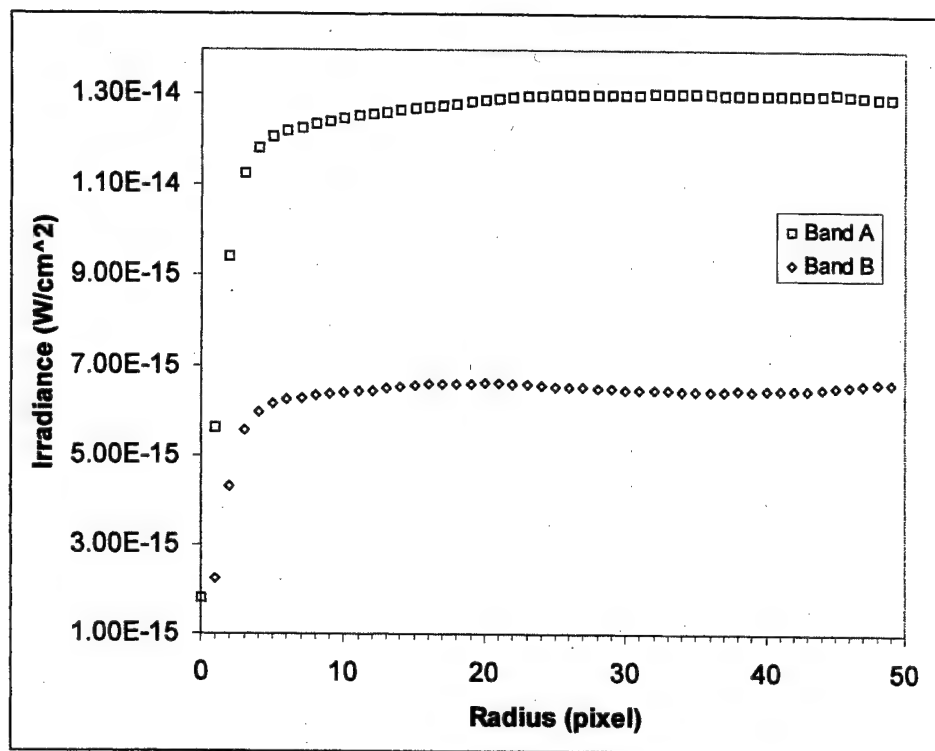
Figure 2. Curves of growth for the star α Boo in CB0605 scar 9. The curves are characterized by a rapid rise of the irradiance within about 4 pixels (36 arcsec) of the center of the image (core of the PRF) followed by a slow rise to about 20 pixels radius (180 arcsec) due to the wings of the PRF, and finally a flat asymptote.
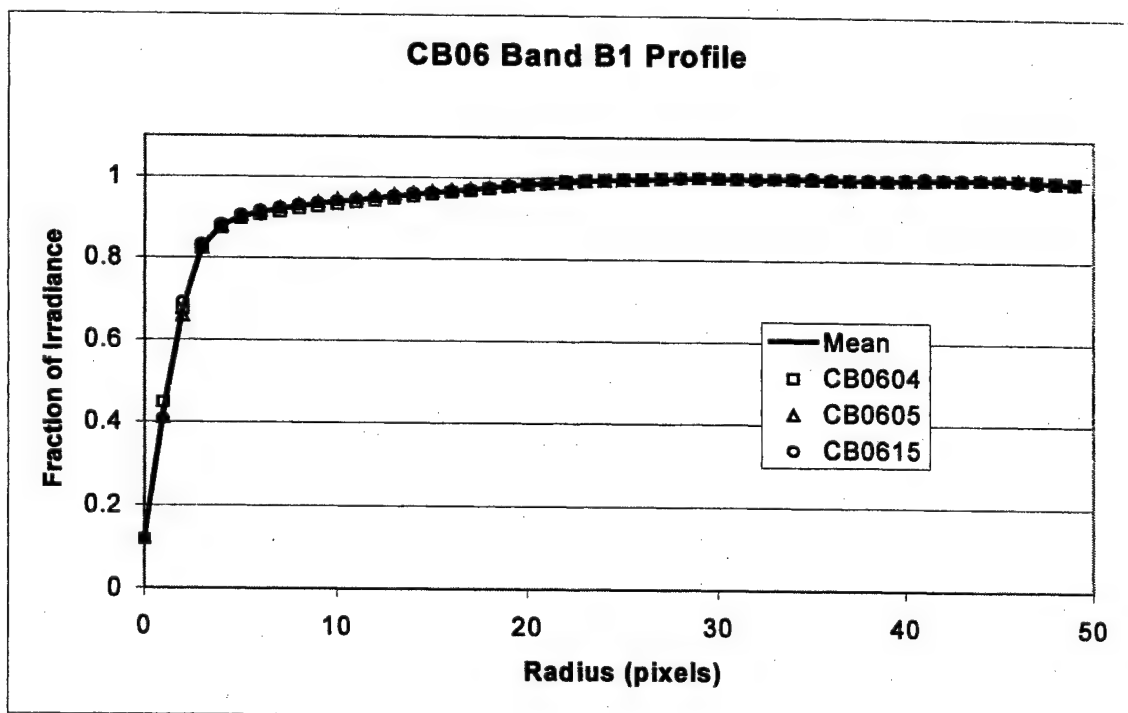
Figure 3. Aperture Photometry Profiles. α Boo is the star in CB0604 and CB0605, while α Tau is the star in CB0615. The plotted points are the means of 16 to 19 scans for each star except for Bands B1 and B2 which are means of 8 to 9 scans.

CB06 Band B2 Profile

CB06 Band C Profile

Figure 3. Aperture Photometry Profiles (continued). α Boo is the star in CB0604 and CB0605, while α Tau is the star in CB0615. The plotted points are the means of 16 to 19 scans for each star except for Bands B1 and B2 which are means of 8 to 9 scans.
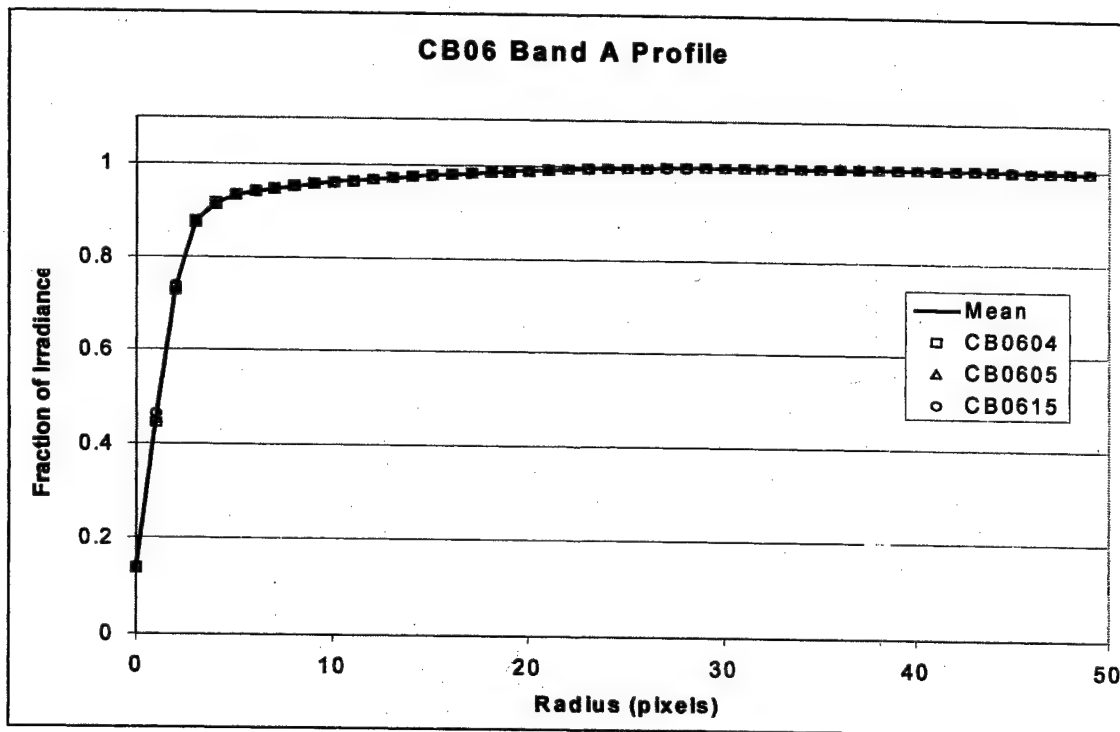
Figure 3. Aperture Photometry Profiles (continued). α Boo is the star in CB0604 and CB0605, while α Tau is the star in CB0615. The plotted points are the means of 16 to 19 scans for each star except for Bands B1 and B2 which are means of 8 to 9 scans.
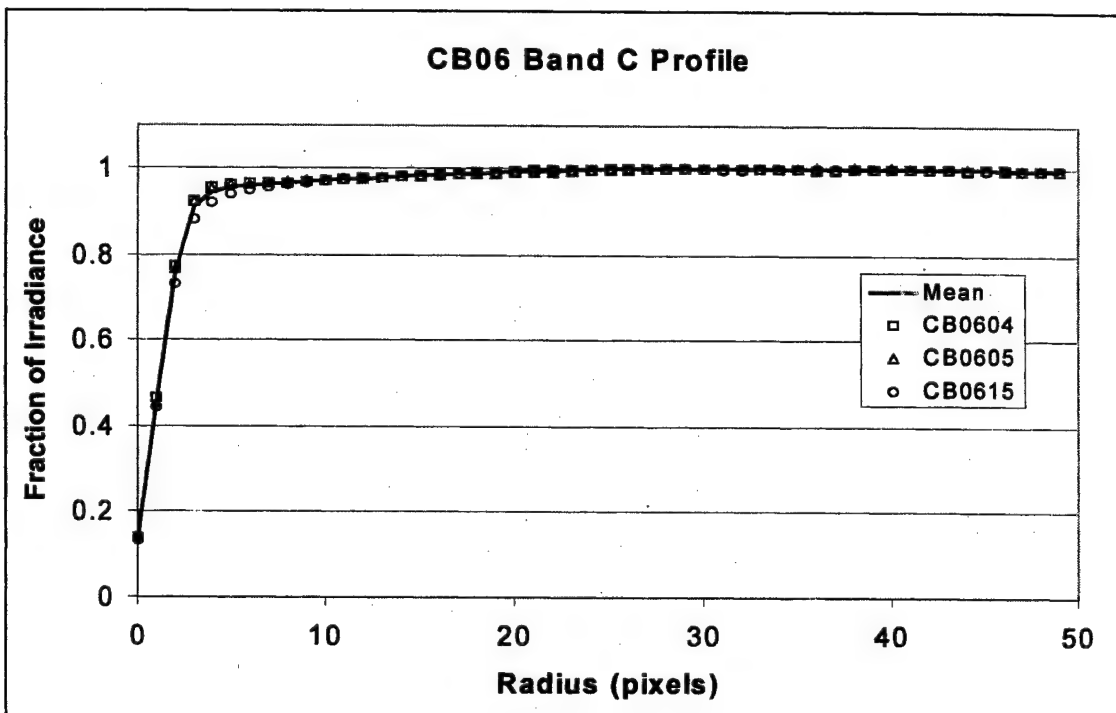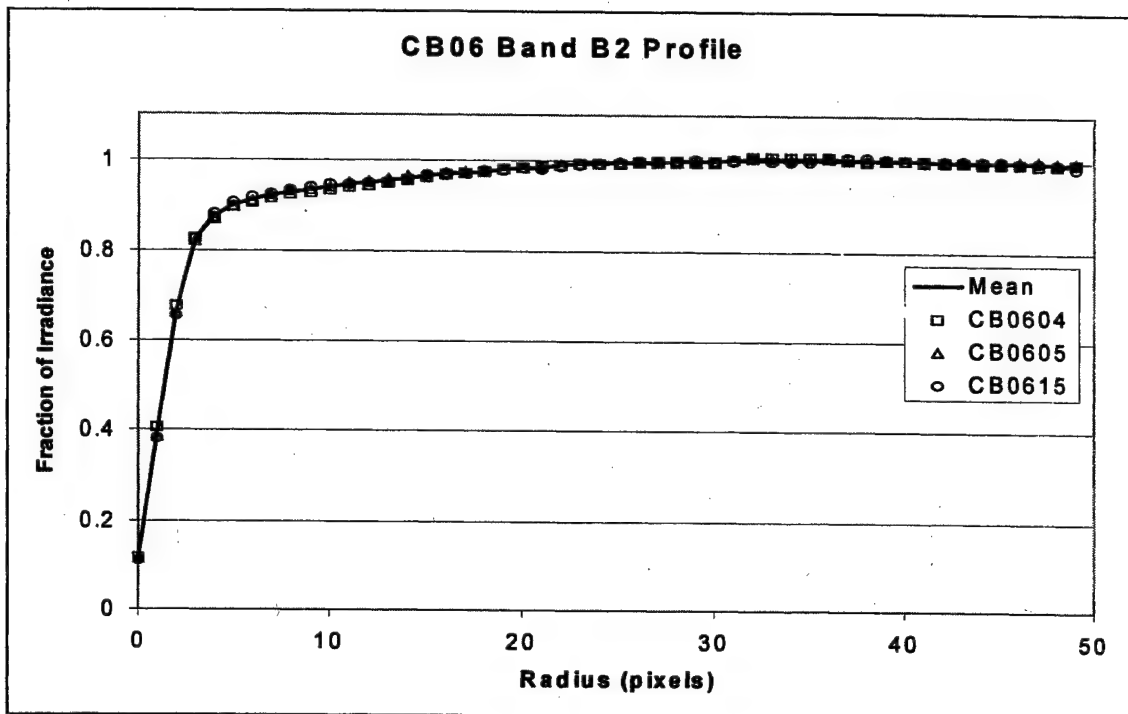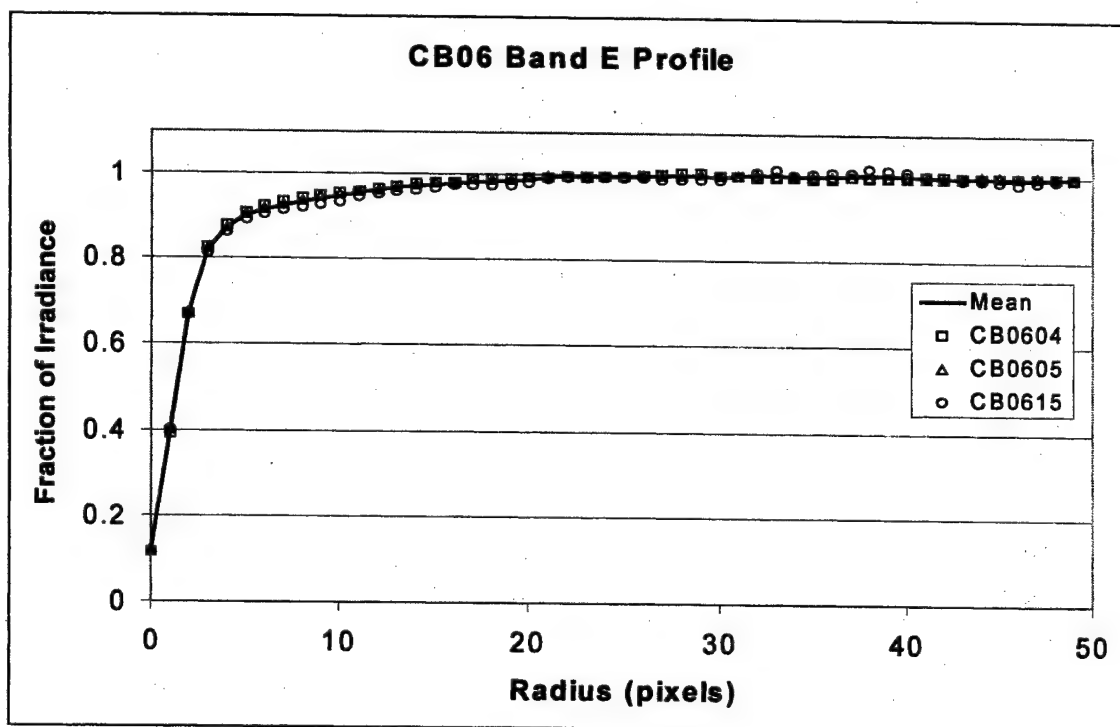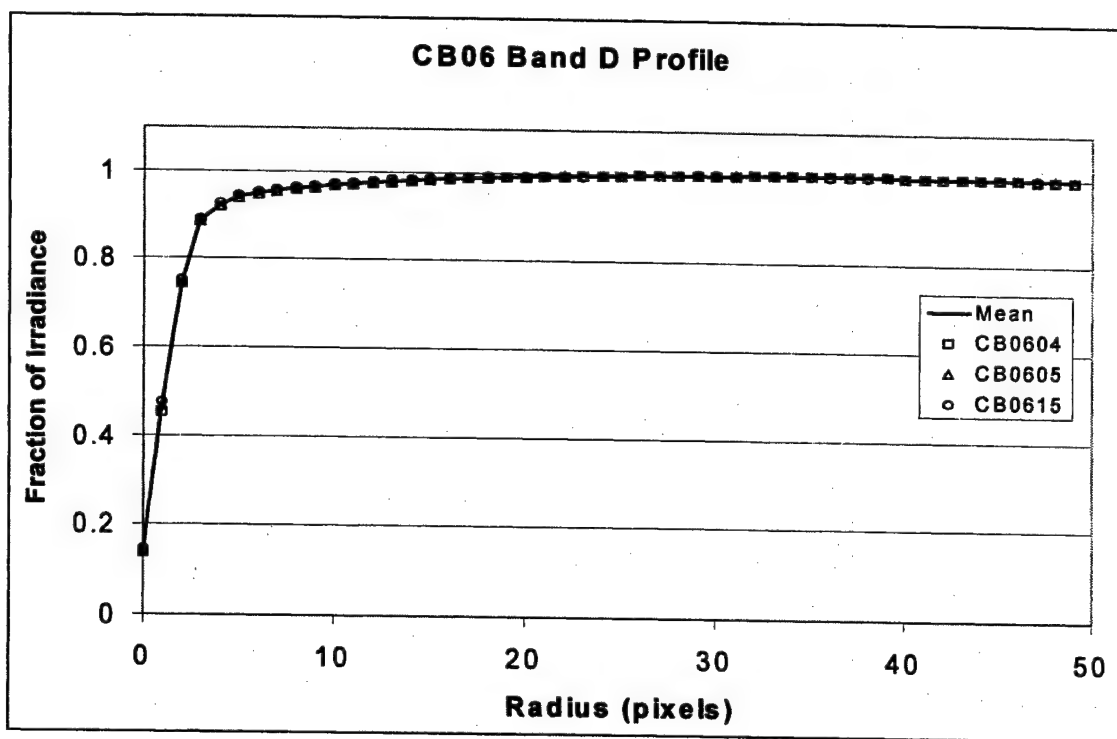
decrease if the residual is negative. To address this problem we iterate the mean baseline to bring the slope of the curve of growth to zero in the region 24 to 50 pixels (216 to 450 arcsec) from the star. Two to three iterations are usually sufficient for convergence to within a small fraction of the noise.

The cleaned 101 x 101 pixel sub-arrays (flux and noise) are saved as FITS images to be used for later coaddition. Pertinent information, such as scan number, name of flux and noise files used, median noise, residual background, source coordinates, irradiance of the target star determined from the curve of growth, the complete curve of growth, and the irradiance from the photometric profile method, are written to a photometry file.

The sub-arrays are then coadded using an interactive program. The program displays the entire set of both flux and noise images of each scan and prompts the operator to choose which scans are to be coadded. Both mean and standard deviation images are produced in the coadd process and archived in FITS format. Aperture photometry is then performed on the target star in the coadded image using the same methods as used on the single scan images. The photometry from the coadded images is our principal result, the photometry of the single scans providing a valuable check on the entire process. Figure 4 shows the coadded images for the same star, α Lyr and the same DCE as shown in the single scan data of Figure 1. The regions depicted in Figure 4 are those used for the aperture photometry.

2.4 Status of the CB06 Analysis

All of our software development is complete, and we have our "pipeline" set up and going. We to date have processed CB0604, 05, 06, 07, 08, 09, 10, 13, 14, 15, and 16 through all steps, that is, CONVERT, POINTING, archive, creation of FITS images, photometry of the images, and coaddition of the data. We must still process CB0617, 18, 19, 20, 21, 22, 23, 24, 25, 26, 31, 32, and 33. Our experience so far is that it takes a minimum of three days to process one DCE if all goes well. On that basis we should complete all the processing by about the first of September.

The next step is absolute calibration and a global solution leading to the final network of MSX calibration stars. We estimate that it will take us about a month to achieve closure - leading to a completion date of this task of about the first of October. A paper describing our results for peer review and publication could be written within a few weeks of that time.
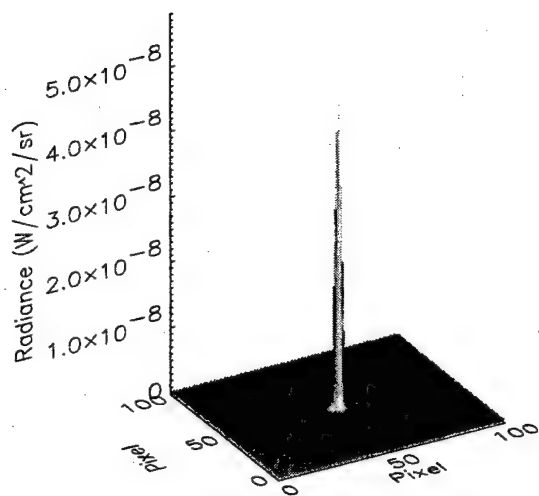
BAND A
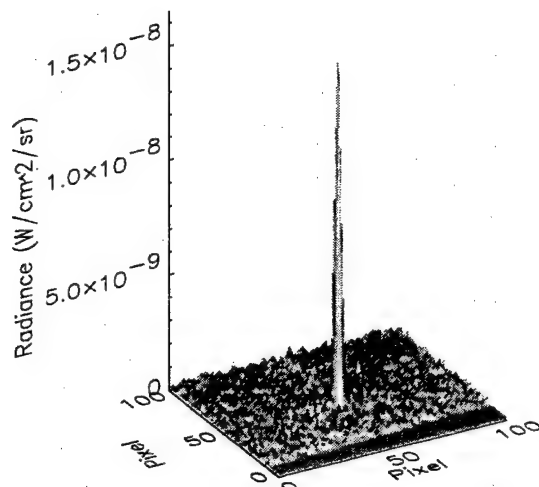
BAND B2
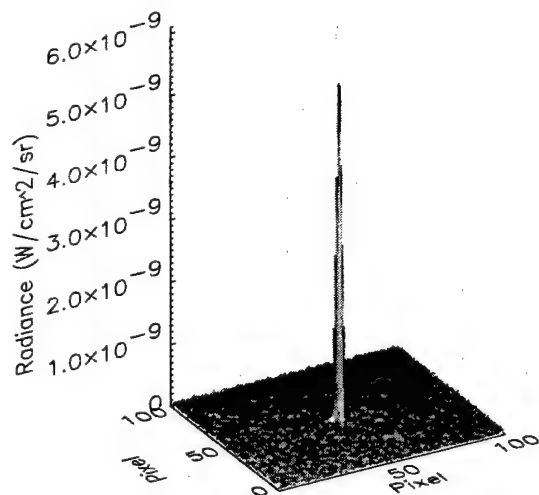
BAND C
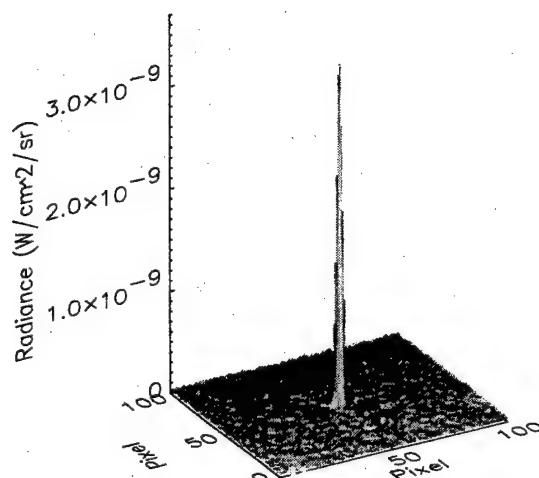
BAND D
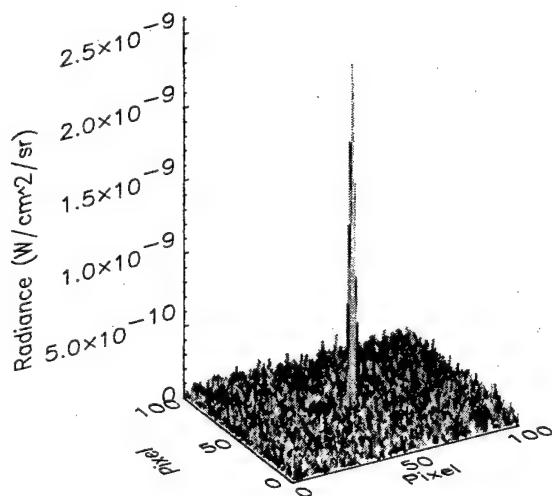
BAND E

Figure 4. Cleaned and coadded images of α Lyr from CB0605. The star is located at pixel (50,50).

12

3. The Air Force Bright Spectral Catalog
3.1 Catalog Definition

It has become clear that current demand for on-orbit calibration of space-based programs, such as SBIRS, requires much brighter calibration sources than are available within the present network. The AFBSC is an independent set of calibrators selected to be among the IR-brightest sources in the sky. Our goal is to create complete (2-35 μm) spectra for all stars brighter than zero magnitude in the mid-infrared. To do this we will utilize IRAS Low Resolution Spectra (LRS), ISO SWS spectra, other groundbased and airborne spectral observations from the past and recent literature, as well as spectra generated by theoretical and/or empirical models.

Candidate stars for the AFBSC are selected from the IRAS all-sky survey, the Cal. Tech. Two Micron Sky Survey, and the MSX point source catalog. For inclusion a star must be brighter than zero magnitude and appear spatially unresolved in the respective survey bands.

The format of the AFBSC is similar to that of the current network of 422 calibration stars, that is, there will be a separate file for each star. The header of the file will contain all the information that we have pertinent to that star, for example:

a) AFBSC identification number,
b) common star names and designations,
c) spectral classification,
d) astrometric coordinates if available,
e) release and revision information,
f) source of the spectral fragments and/or the model spectra used (listed according to the specific wavelength region),
g) photometry used for spectrum normalization,
h) scale factors for fragment normalization,
i) references to the photometry used, and
j) star variability data.

Following the header will be a tabulation of the wavelength, spectral irradiance, uncertainty of the spectral irradiance, and expected range of the irradiance and uncertainty for known variable stars (to be replaced by columns of spectral irradiance versus phase of the variability in later versions of the catalog). We expect that both header and body of the file will become more detailed and complete as the catalog matures.

3.2 Building the Spectra
3.2.1 Approach

Our approach to the AFBSC is a meld of the techniques used to build composites and create templates. Once the list of candidate stars has been assembled we seek spectral fragments from the observational literature, the SKY 4 spectral library, and stellar models. We also seek well characterized photometry from the literature, bring it on to our photometric system, and use it to determine the absolute level of the spectral fragments. The key to the success of this procedure will be in the assignment and tracking of errors throughout the process. In many cases the greatest source of error will be due to our incomplete knowledge of the variability of the source, rather than errors of photometry.

The brighter in the MIR the required calibrators are, the greater the likelihood of encountering abnormal stars such as heavily dust-shrouded, long-period, cool variables. To promote the brighter potential "standards" for IR purposes will require examination of both

optically- and IR-known long-period Mira variables. The key issue is not how stable these are, for they all undergo IR variations, but rather what is known about the variations in IR spectral energy distribution during these radiometric changes. In addition, many of the IR-brightest stars in the sky are so heavily obscured as to be either invisible or extremely faint at optical wavelengths.

3.2.2 Candidate Stars

Table 3 summarizes the search for candidate stars. The bulk of the stars are the 1638 extracted from the IRAS PSC. Of these, we expect that 199 may be dropped (125 HII regions, 70 Planetary Nebulae, 3 t-Tauri stars, and 1 Siefert Galaxy) due to their spatial extent. We are looking at each one for evidence of compactness that might allow them to be retained in the catalog. Many observations of these show obvious beam size effects. Thus the IRAS total will probably be on the order of 1439 sources.

We have found 68 MSX sources in the IRAS gaps that are brighter than 0 mag in any of the SPIRIT III bands. Fifteen of these sources have good IRAS LRS spectra, 5 with multiple observations. All of these sources are in the IRAS working survey database and thus have IRAS names and photometry. This will bring the source total up to 1507. In addition, we have found MSX photometry on 807 of the IRAS sources.

A search of the Two Micron Sky Survey TMSS (Neugebauer and Lieghton, 1969) found 168 stars brighter than $k = 0^m$. A cross-check revealed that 162 were duplicated in the IRAS 1638, yielding only 6 new stars, bringing the source total up to 1513. We also searched the southern extension of the TMSS catalog and found 15 sources, 14 that were duplicated in the IRAS set. The one new star is a fairly normal K5 giant. Thus the final total number of candidate stars is 1514.

Variability dominates the candidate star sample. There are 535 stars listed in the General Catalog of Variable Stars (GCVS) with an additional 160 listed as suspected variables. IRAS found that 920 of the stars had a probability of 99% of being variable at 12 and 25 μm, 992 had a 90% probability, and 1114 had a 50% probability of variability. There are 105 carbon stars and 28 S stars in the sample.

Table 3. Summary of Candidate Stars				
CATALOG	λ (μm)	NUMBER WITH M(λ) ≤ 0	NUMBER EXTENDED	NUMBER IN PSC-2
IRAS PSC-2	12	1638	199	-
IRC	2.2	168	0	162
IRC Extension	2.2	15	0	14
MSX	All Bands	68	0	0

3.2.3 Photometry of the Candidates

Our basic sources of infrared photometry are the IRAS PSC at 12 and 25μm, MSX in the SPIRIT III bands at 4.3, 8.3, 12.1, 14.6, and 21.4 μm, and the Catalog of Infrared Observations (CIO, Gezari, 1993). We plan to augment these sources with additional photometry as the program matures, with particular attention to measurements that will enable studies of the star's variability.

We have found that 1358 of the 1638 AFBSC IRAS sources have additional photometry in the CIO. Also, 375 of our 422 template stars also have photometry in the CIO. This will allow us to bring much of the CIO photometry (193 of 273 references) on to our system in a manner that is similar to our calibration of the IRC (Cohen,et al 1998). The largest single set of photometry in the CIO is the RAFGL 1278 measurements of these stars. Although the uncertainties are large, the RAFGL photometry is quite sufficient to differentiate between multiple spectral shapes possible for many of the objects We have also found that 807 of the 1638 objects have MSX matches and thus photometry in the MSX bands.

We are currently searching the literature for data related to the question of the zero points and calibration standards used by those groups producing the CIO photometry. Of particular interest is the spectral characterization of the bands and detectors used by each. . A total of 1352 papers are cited for the tabulated CIO photometry of our stars, however, many are for measurement of only a few stars. We are focusing on the citations that relate to measurements of 10 stars or more. This limits the list to a more manageable 273 references.

3.2.4 Spectra of the Candidates

Our approach to constructing the spectra of each star is to utilize real observed spectral fragments to the maximum extent. However, the normal situation is that observed fragments covering the complete 2-35 μm spectral range are not usually available. Therefore, we propose to use model and empirical spectra to interpolate between real fragments, and are following multiple paths to acquire the needed spectra.

We have extracted and re-calibrated the average LRS spectra for all the 1638 IRAS sources and 15 MSX stars. This is our basic data set for the 7.7-22.6 μm region. These spectra are expected to be at a good SNR since we are selecting only the brightest sources. It has become clear that in many instances the *average* spectrum has been corrupted by including one or more noisy spectra in the average. In these cases we re-extract the individual spectra and select the appropriate ones to include.

We have also begun looking for spectral variability in the old Groningen LRS archive. A number of our stars have multiple observations spanning the IRAS mission. In particular, two bright Miras in the AFBSC sample - one O-rich, the other C-rich have been compared. Each has 10 viable spectra. The M-Mira showed only level changes over time, with the shape (i.e. the relative contrast of silicate to underlying quasi-continuum) unchanging. The C-Mira showed both level and shape changes (the SiC emission feature changed in contrast with time). Much more of this type of work will be pursued.

We have completed scanning and digitizing the spectral graphs of 125 of our 1638 IRAS selected AFBSC stars that are given in *"Database of Astronomical Infrared Spectroscopic Observations"*, Muizon, Versteege-Hensel, Wisse-Schouten, Duel, and Kessler (1994). We have obtained the original papers for each of these and are in the process of attempting to find out the details of the observations and data reduction, in particular: the standard stars used for reference and the assumptions the authors made about the spectral energy distributions of the standards. We have not yet searched for spectra (other than LRS) of the new MSX gap sources. We have also found an additional 75 spectral fragments in the old NASA ARC database.

In the area of model and empirical spectra, we have created a set of "supertemplates" spanning the wavelength range 0.115 to 35.000 microns for every spectral subclass between

K0 and M2.5III. Model stellar atmospheric spectra have been identified and the archive acquired from Europe to handle "normal" (non-dusty) later M-type giants. We have also created a series of "SKY category" types (with associated SKY3 template spectra from 2-35 microns) for each of the objects.

We are currently in the process of comparing the observed LRS spectra with the postulated template spectra for the assigned SKY source types. This done by a combination of software and visual inspection. MSX photometry and a zero-order reduction of the CIO photometry is used as a guide. Figures 5-15 show some examples of the data used for this comparison. These are not in the form of final spectra, but are work-in-process. A variety of spectra were chosen to show the type of problems that we are dealing with at the present time, as well as to give a sense for the progress we are making. In all the plots: The LRS spectrum is plotted with small "crosses". The LRS was normalized to the IRAS 12μm in-band flux by integration of the spectrum over the 12μm passband. MSX photometry is plotted as "triangles". CIO photometry is plotted as "diamonds". This photometry has had only a cursory zero point correction to bring it to the CWW standard system and thus exhibits large scatter. We will improve this in the future, however, the photometry is sufficient at present to help us differentiate between choices of spectral class (for example: 16079_4812.ps and 17371_3021.ps). The dashed curve is that of the SKY spectrum for the 2503 Classification of that object. The 2503 Class is based on the [12]-[25] and [25]-[60] IRAS colors of the object. This spectrum is normalized to the LRS by a scale factor found by a least squares fit of the spectrum to the LRS data. The solid curve is the spectrum of an automatic "best-fit" classification scheme that we have developed using the SKY spectral library. This spectrum is also normalized to the LRS by a scale factor found by a least squares fit of the spectrum to the LRS data. The IRAS name is at the top of the plot along with the classification of the "best-fit" spectrum. The 2503 Class is indicated at the bottom of the plot. Note that NONE of the photometry has been used (as yet) to constrain the spectra. Some comments about individual spectra:

Figure 5. 06492+0449 – This is a case where the "best-fit" spectrum differs from the 2503 Class. The MSX photometry is in good agreement with the LRS and the extrapolation to shorter wavelengths of the M6G spectrum, as is the CIO photometry. This star is unlikely to vary significantly in the IR.

Figure 6. 06500+0829 - This is a case where the "best-fit" spectrum coincides with that from the 2503 Class, although the fit is not very good. The extension of the spectrum to short wavelengths is consistent with the CIO photometry. The position of the MSX photometry (taken 13 years later than the LRS) indicates that this star is probably highly variable in both amplitude and spectral shape, the highest degree of variability being at the shortest wavelengths.

Figure 7. 12544+6615 – Again this is a case where the "best-fit" spectrum coincides with that from the 2503 Class. Although there is no MSX photometry of this object, the extrapolated spectrum is in good accord with the CIO photometry. The upper points near 8 and 11 microns might indicate some variability.
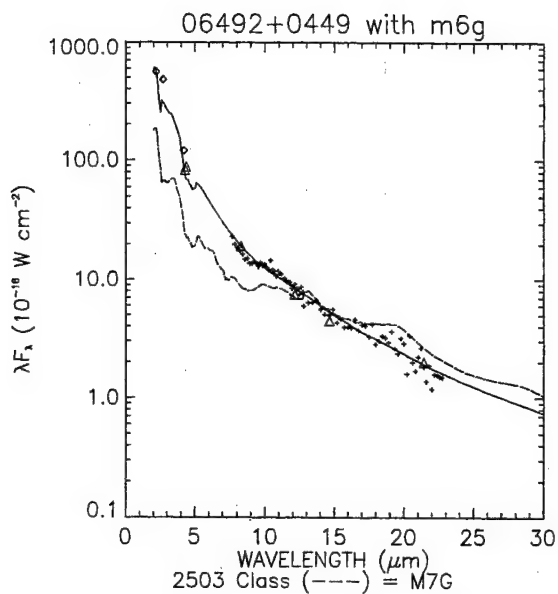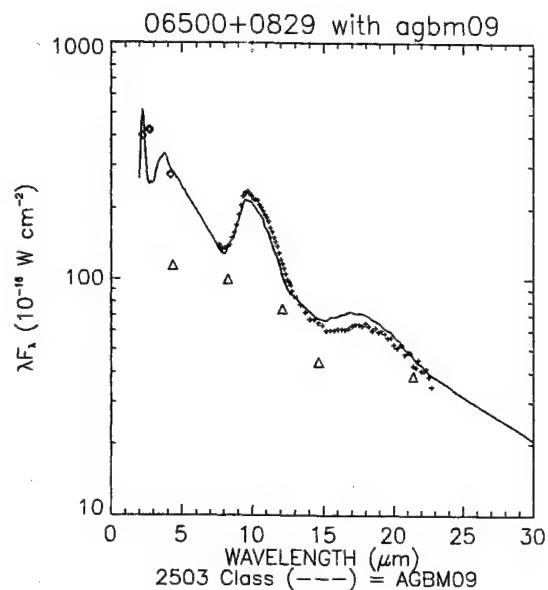
Figure 5. Spectral classification and fit data.

Figure 6. Spectral classification and fit data.

Figure 7. Spectral classification and fit data.

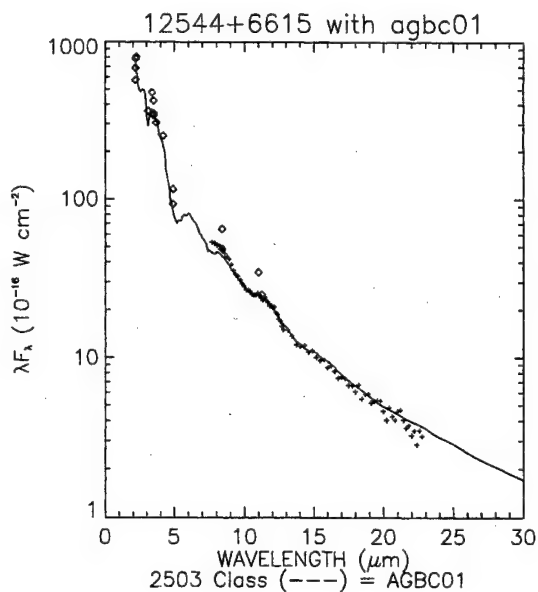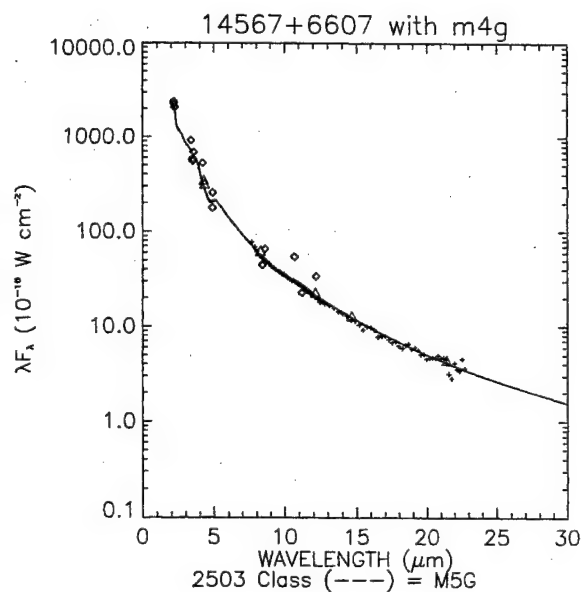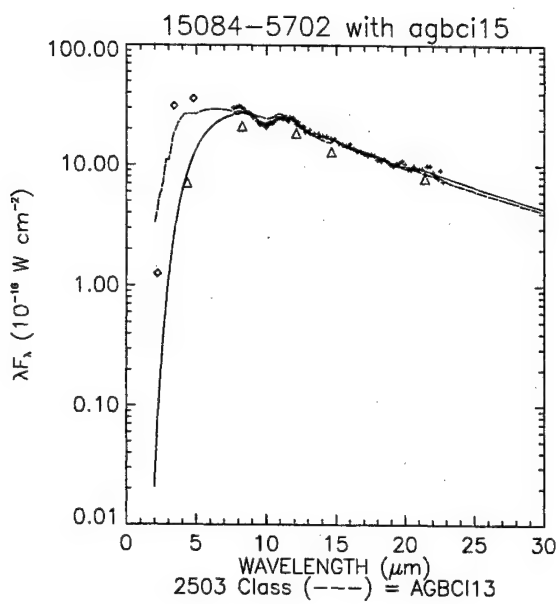**Figure 8. Spectral classification and fit data.**

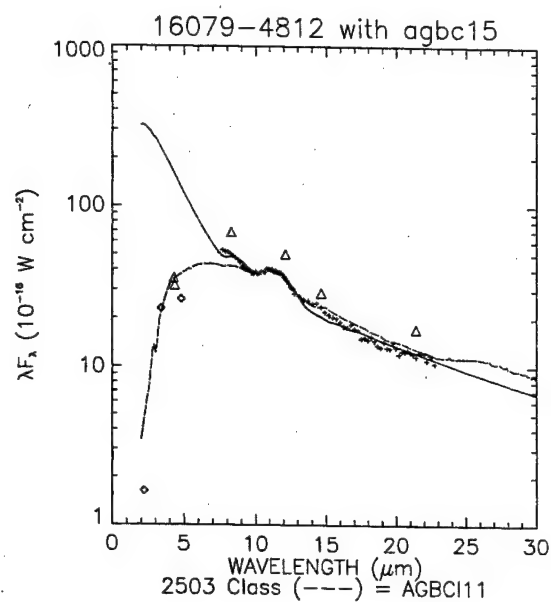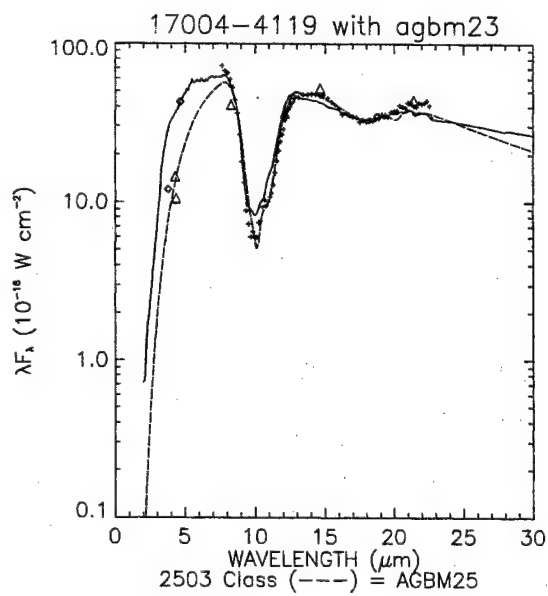Figure 9. Spectral classification and fit data.

Figure 10. Spectral classification and fit data.
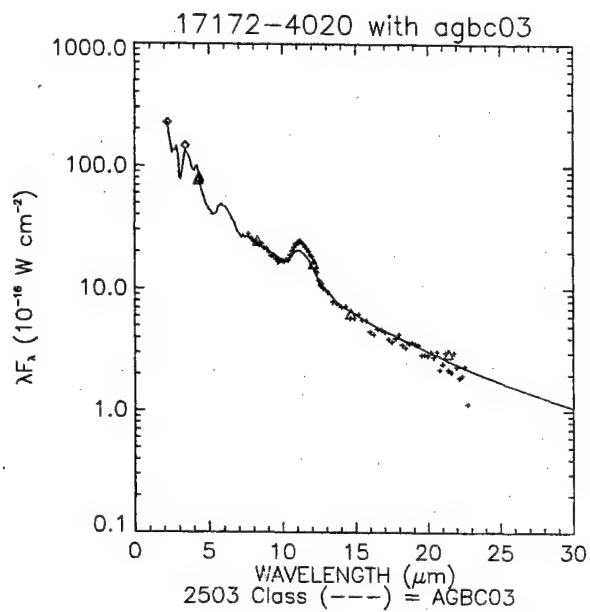

Figure 11. Spectral classification and fit data.

Figure 12. Spectral classification and fit data.
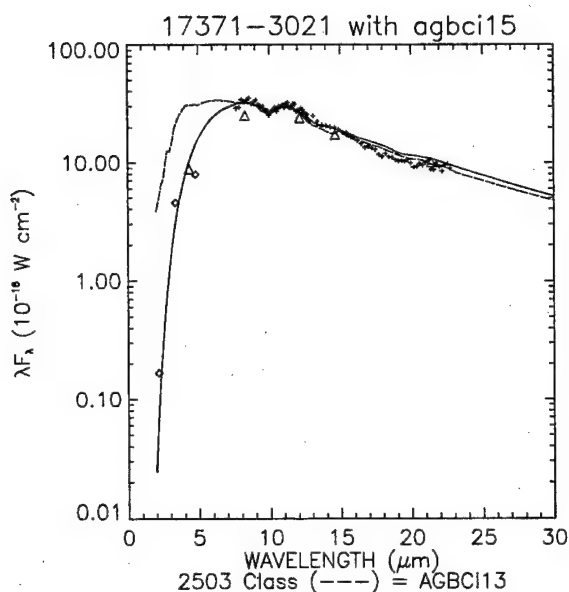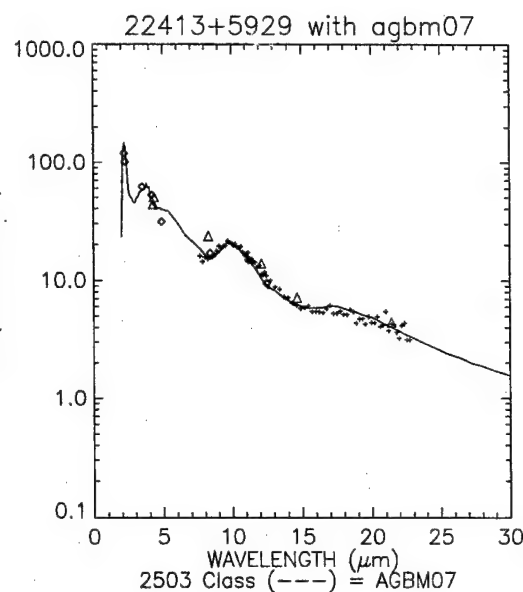
18

Figure 13. Spectral classification and fit data.

Figure 15 Spectral classification and fit data.
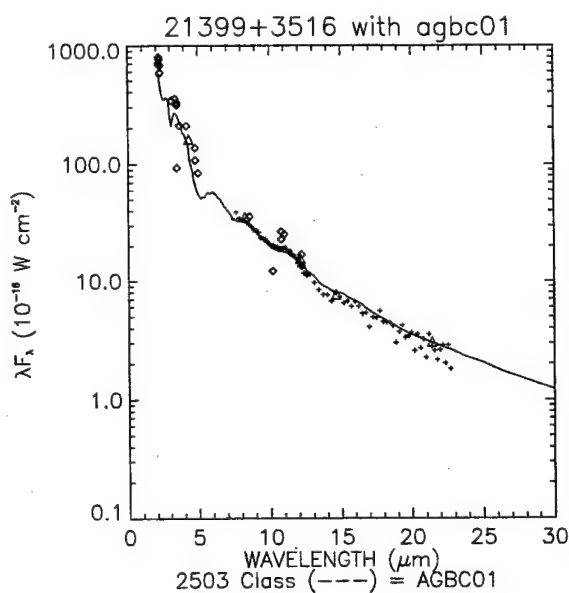
Figure 14. Spectral classification and fit data.

Figure 8. 14567+6607 – It is clear in this plot that the differences between M4G and M5G cannot be resolved on this scale. Both spectra are in good agreement with the photometry.

Figure 9. 15084-5702 – Here the star is certainly varying in both amplitude and spectral shape. The highest degree of variability being apparently at the shortest wavelengths.

Figure 10. 16079-4812 – As mentioned above, this is a good example of photometry constraining the range of spectral type.

Figure 11. 17004-4119 – This is a good example of a source with extreme silicate absorption. The MSX photometry favors the 2503 Class. The CIO photometry at 4.2 um is the AFGL value taken at quite a different epoch and favors the "best-fit" classification.

Figure 12. 17172-4020 – Another example of reasonable extrapolation to shorter wavelengths.

Figure 13. 17371-3021 - Extrapolation of AGBCi15 over a large dynamic range, and as mentioned above, is another good example of photometry constraining the range of spectral types.

Figure 14. 21399+3516 – A spectrum well constrained by LRS, MSX and CIO.

Figure 15. 22413+5929 - Another spectrum well constrained by LRS, MSX and CIO. These kind of data give us a warm feeling as to the credibility of the methods we are developing.

3.2.5 Ground Based Spectral Observations

We had initially hoped to form a cooperative program to secure new spectra of a selected set of these objects. The selected stars would be observed at least four times a year until a major part of their periods had been sampled. This was be accomplished using the NASA Ames HIFOGS spectrometer at the Wyoming IR Observatory (WIRO). Observations would be obtained by the collaborating group, while our effort would be reduction and analysis of the spectra.

The uncertainty as to the potential demise of the Wyoming Physics Dept. has terminated the special relationship between NASA-Ames and WIRO. Therefore, our anticipated collaboration with D. Wooden of NASA-Ames (to secure quarterly 8-13 micron spectra of a handful of carefully selected Mira variables in the AFBSC) has also ended after a single run plagued by constant bad weather conditions.

However, papers are beginning to appear in the literature that document long-term (several year) programs of monitoring of some of the brightest AFBSC stars. Further, complete ISO SWS spectra are also appearing at conferences and in the literature that indicate the character of spectral variations around some Mira cycles. Therefore, we will probably replace our intended ground-based effort to secure IR spectra in just one "window" by a perusal of both the complete AOT-1 SWS spectral showing variations around a give star's cycle, and of the technique used by the Japanese to model the actual variations of a single star around its cycle. Longer term efforts are still ongoing in Vienna to create dynamical atmospheres with full radiative transfer treatment and thereby predict the plausible spectral variability of individual stars.

3.3 Status of the AFBSC

We now have enough data in-hand to consider production of a preliminary version of the AFBSC. This version would be confined to those stars that we feel confident variability will not play a major factor, and /or those stars to which we can assign meaningful (although perhaps large) spectral irradiance uncertainties. This set would be then available as a guide to what can be expected from the full catalog, and offer an opportunity for users to discover its shortcomings. We feel confident that a Version 1.0 AFBSC could be completed by the first of the year.

REFERENCES

Cohen, M., Walker, R.G., Barlow. M.J., and Deacon, J.R., 1992, "Spectral Irradiance Calibration in the Infrared, I. Groundbased and IRAS Broadband Calibrations," *Astron. J.* **Vol 104**, No.4, 1650-1657.

Cohen, M., Walker, R.G. and Witteborn, F., 1992, "Spectral Irradiance Calibration in the Infrared, II. Alpha Tau and the Recalibration of the IRAS Low Resolution Spectrometer," *Astron. J.* **Vol 104**, No.5, 2030-2044.

Cohen, M., Witteborn, F.C., Carbon, D.F., Augason, G.C., Wooden, D., Bregman, J.D., & Goorvitch, D. 1992, "Spectral Irradiance Calibration in the Infrared, III. The Influence of CO and SiO," *Astron. J.*, **Vol 104**, p2045

Cohen, M., Witteborn, F.C., Walker, R.G., Bregman, J.D., and Woden, D.H., 1995, "Spectral Irradiance Calibration in the Infrared, IV. 1.2-35 Micron Spectra of Six Standard Stars," *Astron. J. ,* **Vol 110**, no. 1

Cohen, M. & Davies, J.K., 1995, "Spectral Irradiance Calibration in the Infrared, V. The Role of the UKIRT and the CGS3 Spectrometer," *Monthly Notices of the Royal Astronomical Society*, **V275**, p715

Cohen, M., Witteborn, F.C., Bregman, J.D., Wooden, D.H., Salama, A., & Metcalfe, L. 1996, "Spectral Irradiance Calibration in the Infrared, VI. Three Southern Standards," *Astron. J.*, **V112**, p241

Cohen, M., Witteborn, F.C., Carbon, D.F., Davies, J.K., Wooden, D.H., & Bregman, J.D. ,1996, "Spectral Irradiance Calibration in the Infrared, VII. New Composite Spectra, Comparisons with Model Atmospheres, and Far-IR Extrapolations," *Astron. J.*, **V112**, p2274

Cohen, M., Witteborn, F.C., Roush, T., Bregman, J.D. & Wooden, D.H., 1998, "Spectral Irradiance Calibration in the Infrared, VIII. 5-14 Micron Spectroscopy of the Asteroids Ceres, Vesta, and Pallas," *Astron. J.*, **V115**, p1671

Cohen, M., 1998, "Spectral Irradiance Calibration in the Infrared, IX., Calibrated Stellar Spectra Using DIRBE Radiometry," *Astron. J.*, **V115**, p2092

Cohen, M., Walker, RG, Carter, B., Hammersley, P., Kidger, M. and Noguchi, K., 1999, "Spectral Irradiance Calibration in the Infrared. X. A Self-Consistent Radiometric All-Sky Network of Absolutely Calibrated Stellar Spectra," *Astron. J.*, **V117**, 1864-1889

Murdock, T. L. 1997, "Preliminary Analysis of the MSX Calibration Sphere Data," presentation to ISO Calibration Working Group, March 13, 1997

Neugebauer, G., and Leighton, R.B., 1969, "Two Micron Sky Survey Catalog," NASA SP-3047 – available on NASA NSSDC CD ROM, Selected Astronomical Catalogs, Vol.1, No. 1

Walker,R.G,1998, "SPIRIT III On Orbit Calibration and Data Analysis, Reduction and Analysis of Data Certification and Technology Transfer Experiment,DC34 - Flat Field Calibration, Earthlimb Mode", Final Report on Subcontract C916614, Part 3 (Space Dynamics Laboratory,Logan, UT)

APPENDIX A. THE NOISE ESTIMATOR

The noise in a data stream, x_i, is defined as the square root of the variance, σ^2, that is

$$\sigma^2 = (1/n) \sum (x_i - x_m)^2, \tag{1}$$

where x_m is the mean of x, and the sum is over n samples. If we define $y_i = x_i - x_m$, then

$$\sigma^2 = (1/n) \sum y_i^2. \tag{2}$$

It is not always easy to determine the mean of the signal in a long scan due to real variations in the background and embedded sources of radiance. To reduce the effects of background variations we have adopted the following scheme to estimate the noise. Define the quantity Ω as

$$\Omega^2 = (1/n) \sum (x_i - x_{i+1})^2 \tag{3}$$

which by the above substitution yields

$$\Omega^2 = (1/n) \sum ((y_i + x_m) - (y_{i+1} + x_m))^2 = (1/n) \sum (y_i - y_{i+1})^2 \tag{4}$$

expanding the sum we have

$$\Omega^2 = (1/n) \sum y_i^2 + (2/n) \sum y_i y_{i+1} + (1/n) \sum y_{i+1}^2 \tag{5}$$

The central term of equation (5) is the covariance of y, which for y random is zero. Also, for a reasonable number of samples, the sum of y_i^2 will be equal to the sum of y_{i+1}^2 for y random. Thus we have

$$\Omega^2 \approx (2/n) \sum y_i^2 = 2 \sigma^2 \tag{6}$$

To estimate the pixel noise, the above was implemented as follows:

a) Convolve the data samples with the kernel [-1.0, +1.0]. This is equivalent to taking the difference in equation (3).
b) Square the resulting vector.
c) Smooth the squared vector with a running boxcar integration of 101 samples and divide by 2. Thus we are calculating the noise at each data sample using 101 points centered on the sample.
d) Take the square root to calculate the noise at every pixel sample.
e) Calculate the median of the resulting noise vector to reduce the sensitivity to the presence of discrete sources of radiance (stars, etc). The assumption here is that the noise is reasonably constant during the scan, and the purpose of estimating the noise is to characterize it with respect to the noise from other pixels. The principal use of the estimated noise is for statistical weighting of the pixel samples.

Symbols, Abbreviations, and Acronyms

AFBSC	Air Force Bright Spectral Catalog
AFGL	Air Force Geophysics Laboratory
CIO	Catalog of Infrared Observations
DAF	Definitive Attitude Files
DCE	Data Collection Event
DEC	Declination
DOD	Department of Defense
ESA	European Space Agency
GCVS	General Catalog of Variable Stars
IDL	Interactive Data Language
IR	Infrared
IRAS	Infrared Astronomical Satellite
IRTS	Infrared Telescope in Space
ISO	Infrared Space Observatory
LRS	Low Resolution Spectra
MIR	Mid Infrared
MSX	Midcourse Space Experiment
NASA	National Aeronautics and Space Agency
PL DAC	Philips Laboratory Data Analysis Center
PRF	Point Response Function
PSC	Point Source Catalog
RA	Right Ascension
RAFGL	Revised Air Force Geophysics Laboratory
SCIES	Science Catalog Information Exchange System
SNR	Signal to Noise Ratio
SPIRIT III	Spectral Infrared Interferometric Telescope III
SWS	Short Wavelength Spectrometer
TMSS	Two Micron Sky Survey
WIRO	Wyoming Infrared Observatory